Supporting Information

Bioactive multifunctional dressing with simultaneous visible monitoring pH value and H_2O_2 concentration for promoting diabetic wound healing

Jimin Huang, Jinzhou Huang, XinXin Zhang, Qinyi Xie, Yi Zheng, Chaoqin Shu, Zhe Shi, Xiao Wang, Jiajie Chen, Bing Ma, Chengtie Wu, Yufang Zhu [*]

[a] State Key Laboratory of High Performance Ceramics and Superfine Microstructure
Shanghai Institute of Ceramics, Chinese Academy of Sciences
1295 Dingxi Road, Shanghai 200050, P.R. China
[*] Prof. Yufang Zhu, Email: zjf2412@163.com

[b] Center of Materials Science and Optoelectronics Engineering
University of Chinese Academy of Sciences
19A Yuquan Road, Beijing 100049, P. R. China

[c] School of Pediatrics, Chongqing Medical University
136 Zhongshan 2nd Road, Chongqing 400014, P. R. China

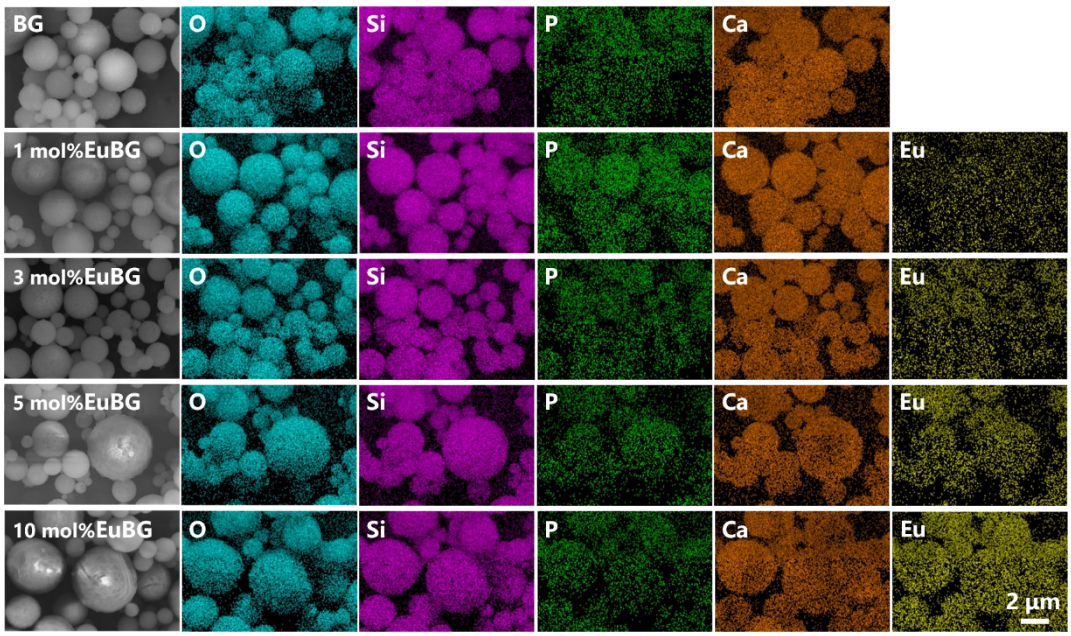

Figure S1. SEM-EDS elemental mappings of x mol%EuBG particles (x=0, 1, 3, 5, 10).

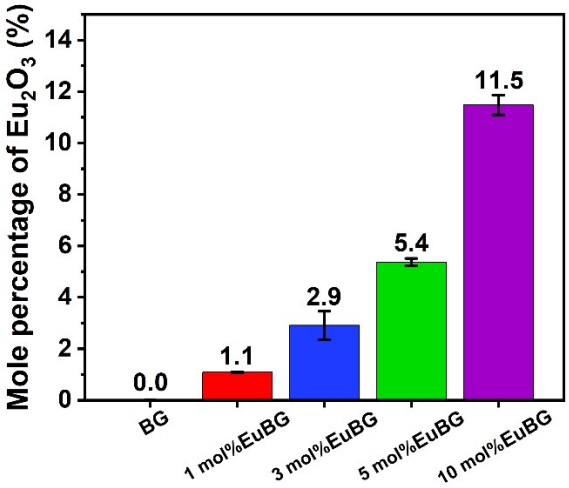

Figure S2. Actual mole percentage of Eu_2O_3 in x mol%EuBG particles obtained by ICP testing (x=0, 1, 3, 5, 10).

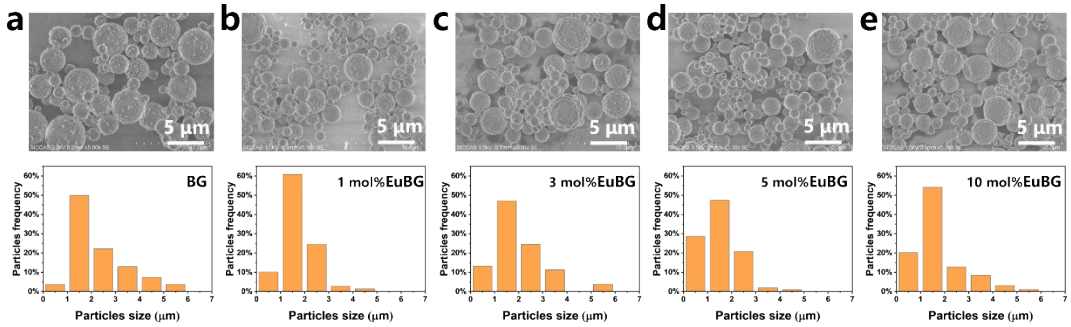

Figure S3. Particle size distribution of x mol%EuBG particles (x=0, 1, 3, 5, 10) obtained by ImageJ statistics.

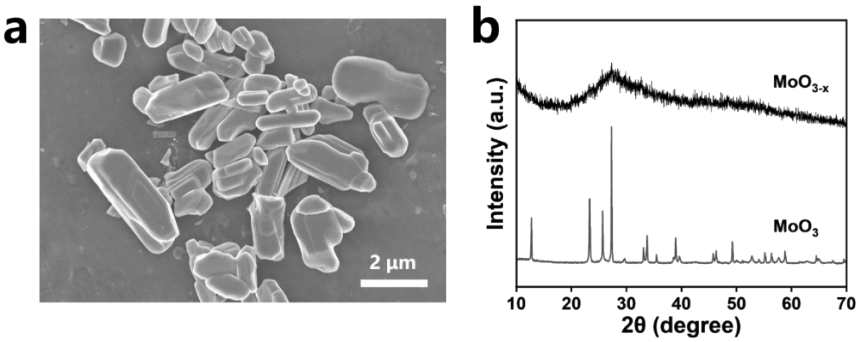

Figure S4. (a) SEM image of MoO_3 powders. (b) XRD patterns of MoO_3 powders and MoO_{3-x} nanosheets.

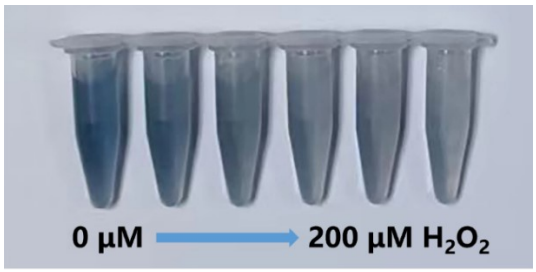

Figure S5. Visible color changes of the MoO_{3-x} nanosheet solutions with different concentration of H_2O_2 (0-200 μmol L^{-1}).

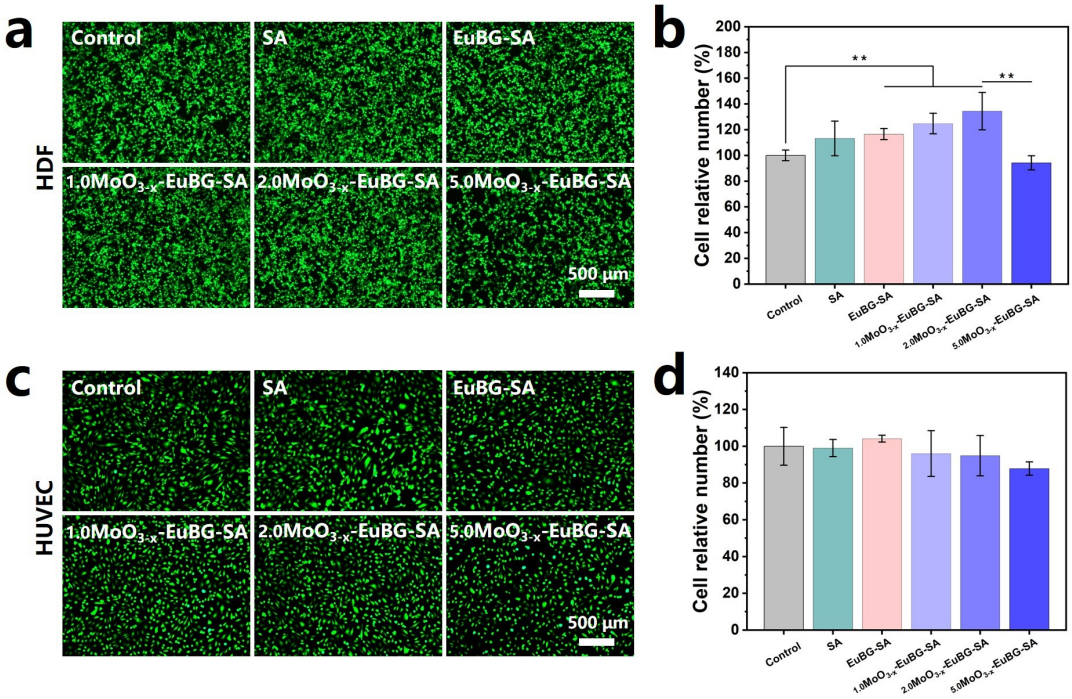

Figure S6. Live/dead staining images and corresponding cell relative number of (a, b) HDFs and (c, d) HUVECs (n=4). All data are expressed as means ± standard deviation, one-way ANOVA with Bonferroni multiple comparison corrections, **p < 0.01.

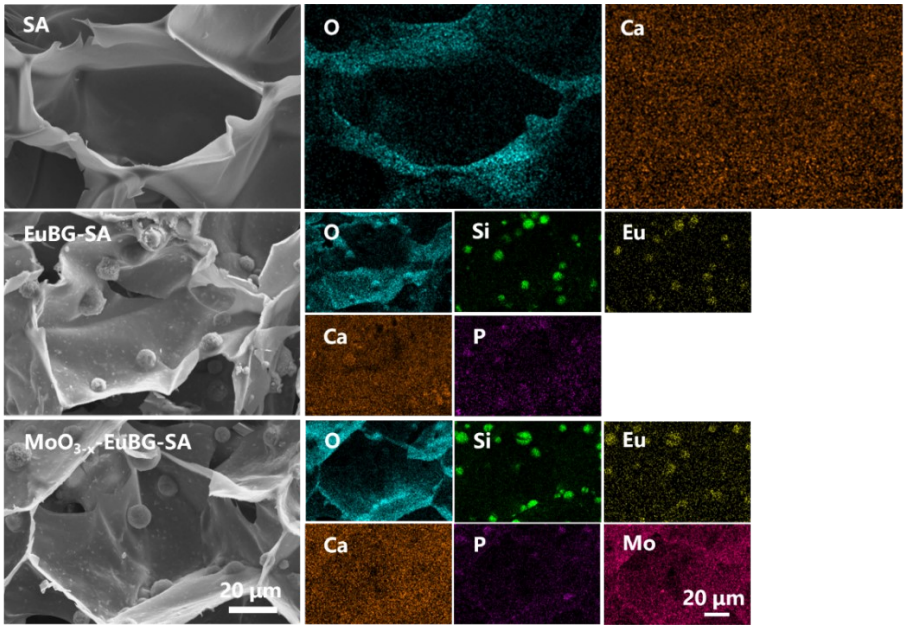

Figure S7. SEM-EDS elemental mappings of the inside of SA, EuBG-SA, and MoO_{3-x}-EuBG-SA dressings.

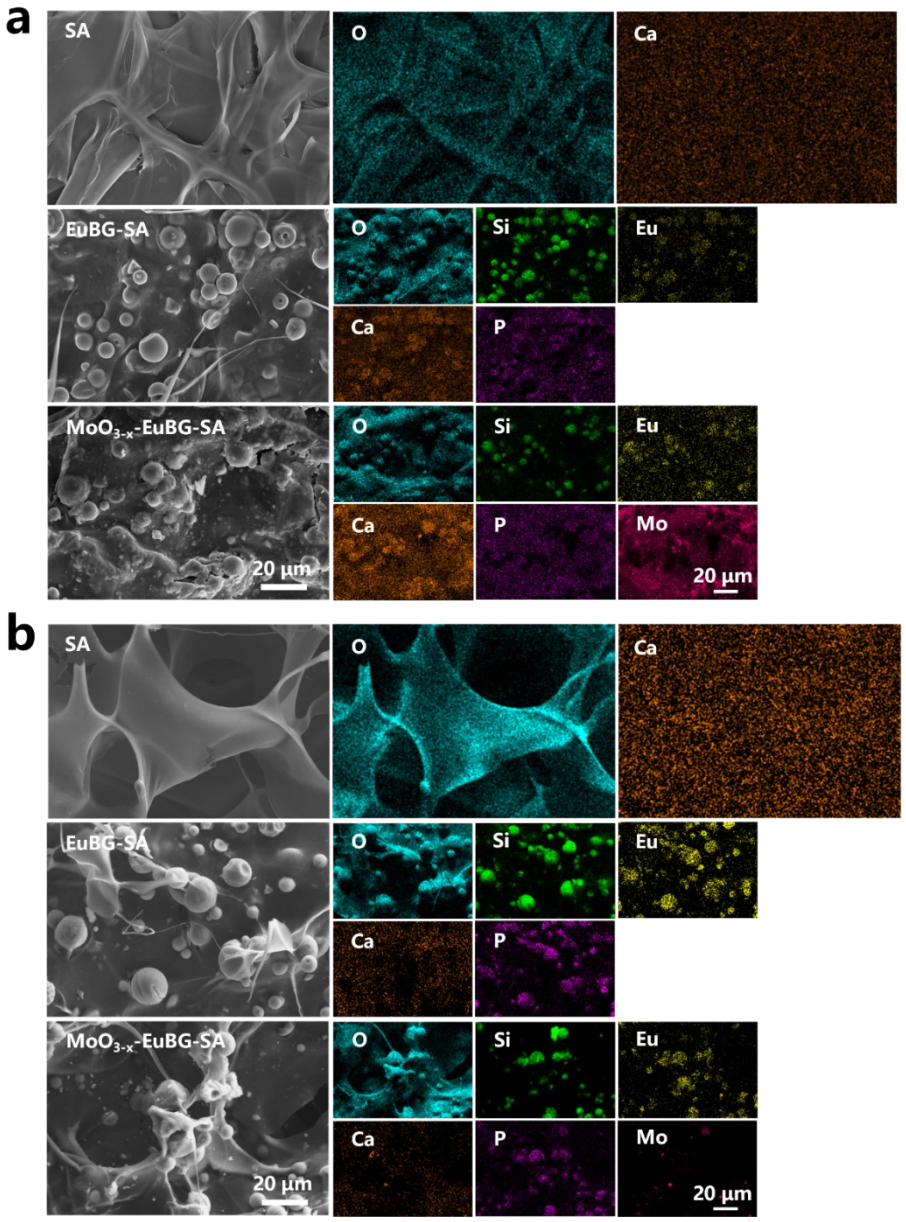

Figure S8. SEM-EDS elemental mappings of the surface of SA, EuBG-SA, and MoO_{3-x}-EuBG-SA dressings (a) before and (b) after immersing in Tris-HCl (pH=7.4) for 5 days.

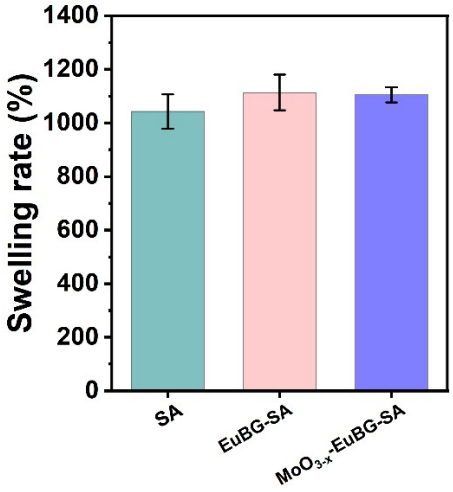

Figure S9. The swelling rate of SA, EuBG-SA, and MoO_{3-x}-EuBG-SA dressings (n=6). All data are expressed as means ± standard deviation.

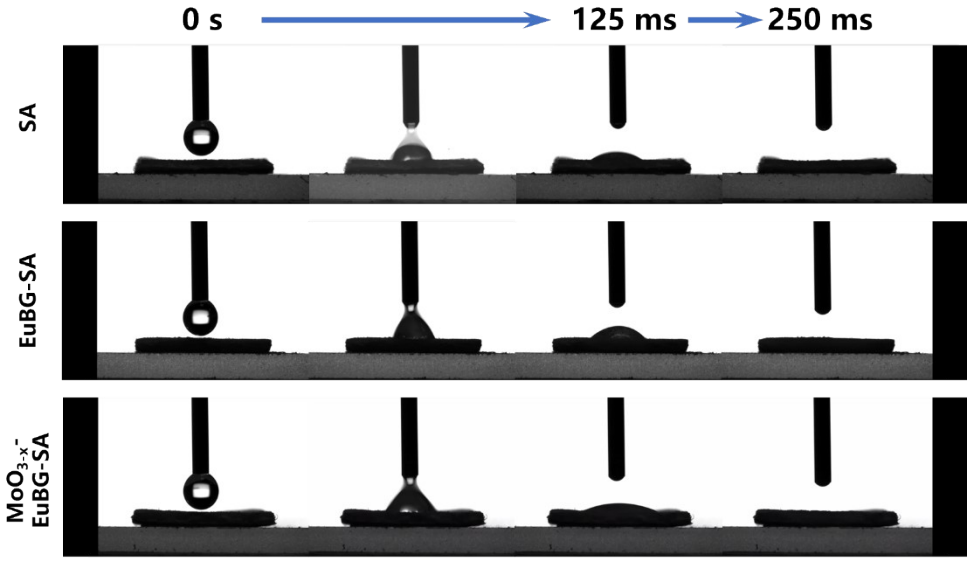

Figure S10. Hydrophilicity tests of SA, EuBG-SA, and MoO_{3-x}-EuBG-SA dressings.

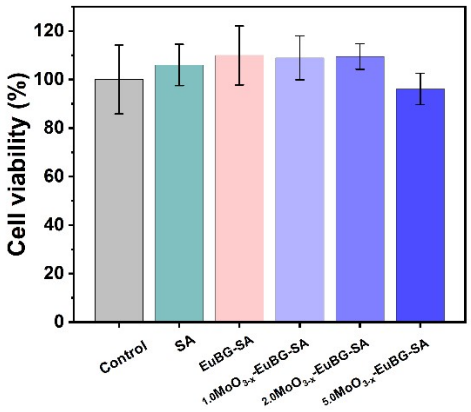

Figure S11. Cell viability of RAW 264.7 cultured with MoO_{3-x}-EuBG-SA dressings, (n=5). All data are expressed as means ± standard deviation.

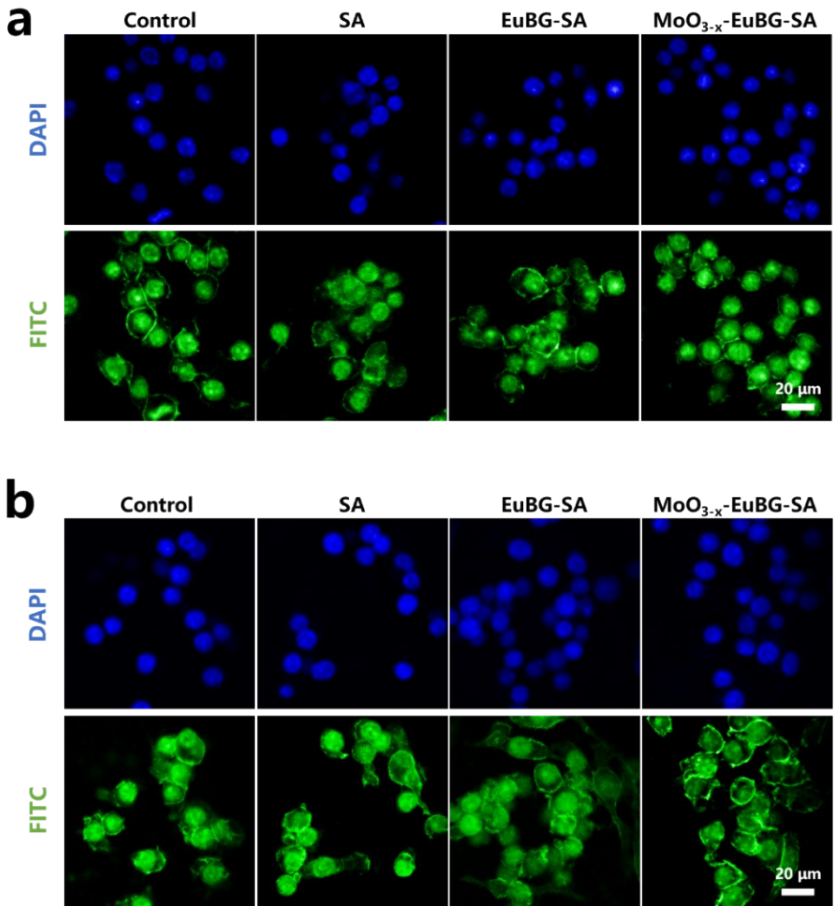

Figure S12. The representative (a) Arg-1 and (b) TNF-α fluorescence images of the RAW 264.7 cells (blue: cell nuclei; green: cytoskeleton).

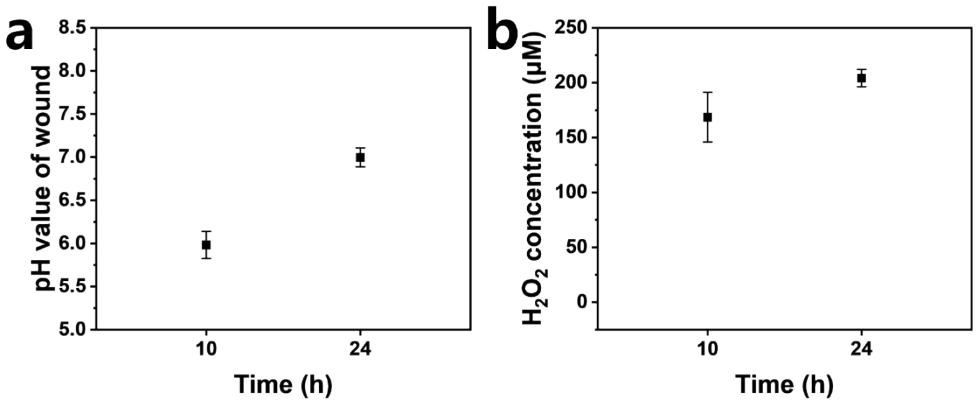

Figure S13. pH value and H_2O_2 concentration of mice wound, n=4. All data are expressed as means ± standard deviation.

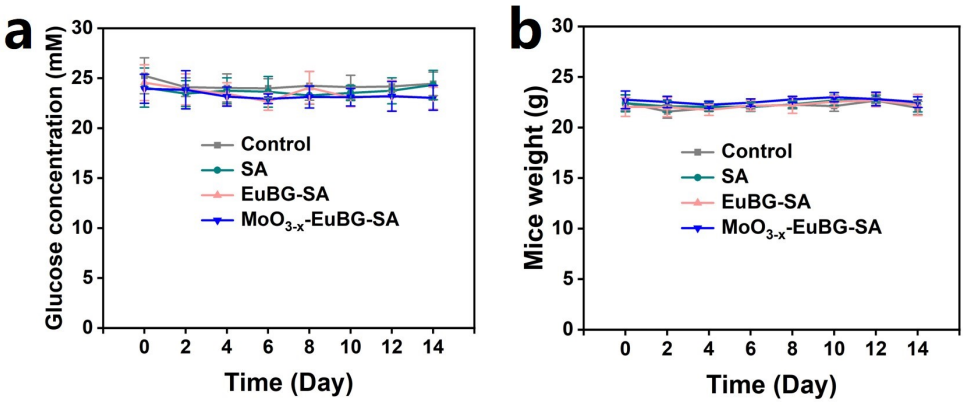

Figure S14. (a) Glucose concentrations in blood and (b) diabetes mice weight from day 0 to day 14 after injury (n=5). All data are expressed as means ± standard deviation.

Table S1. Primers sequences for RT-qPCR.

Gene	Primer sequence
GADPH F	GATTTGGTCGTATTGGGCG
GADPH R	CTGGAAGATGGTGATGG
VEGF F	TATGCGGATCAAACCTCACCA
VEGF R	CACAGGGATTTTTCTTGTCTTGCT
HIF-1α F	ATCCATGTGACCATGAGGAAAT
HIF-1α R	CTCGGCTAGTTAGGGTACACTT
bFGFR F	GACGGCTCCTACCTCAA
bFGFR R	GCTGTAGCCCATGGTGTTG

Table S2. Primers sequences for RT-qPCR.

Gene	Primer sequence
GADPH F	AGAACATCATCCCTGCATCCAC
GADPH R	TCAGATCCACGACGGACACA
TNF-α F	CTGTAGCCCACGTCGTAGCAA
TNF-α R	TGTCTTTGAGATCCATGCCGTT
iNOS F	CAGAAGTGCAAAGTCTCAGACAT
iNOS R	GTCATCTTGTATTGTTGGGCT
Arg-1 F	AACCTTGGCTTGCTTCGGAACTC
Arg-1 R	GTTCTGTCTGCTTTGCTGTGATGC
CD206 F	ATCCACGAGCAAATGTACCTCA
CD206 R	TAGCCAGTTCAGATACCGGAA